Microwave System for Breast Tumor Detection

E. C. Fear, *Student Member, IEEE,* and M. A. Stuchly, *Fellow, IEEE*

***Abstract*— A preliminary numerical analysis of a system for breast tumor detection, amenable to practical implementation, is described. The general idea was previously introduced and relies on ultrawide-band radar and confocal imaging. The system consists of an array of small antennas placed away from the breast. Simulations of each antenna in the array are performed with the finite-difference time-domain (FDTD) method. A tumor detection algorithm is applied to the data, incorporating skin return subtraction to enhance tumor returns.**

***Index Terms*—Microwave imaging, tumor detection, ultrawide-band radar.**

I. Introduction

BREAST cancer affects many women, and early detection is an important part of management of this disease. Mammography, which exposes women to ionizing radiation, is typically used in breast imaging. Microwaves have the potential to provide effective tumor detection due to the difference in dielectric properties of normal breast tissue and breast tumors at microwave frequencies. Previously proposed systems for microwave imaging reconstruct object profiles from measured scatter of a narrowband illumination signal by the object. Early systems employed diffraction tomography in reconstruction which did not provide adequate images. More recent systems use iterative nonlinear inverse-scattering approaches, providing improved images but requiring computationally intensive image reconstruction [1], [2]. A new concept introduced by Hagness *et al.* uses a pulsed microwave confocal system to detect tumors [3], [4]. The ideas are closely related to optical confocal systems, however microwaves offer better penetration depth in tissue. Time-shifting recorded signals creates synthetic focal points. Returns from scatterers at the focal point add coherently, while returns from scatterers off focus add incoherently and are suppressed. Both two- and three-dimensional (2-D and 3-D) simulations were performed with the finite-difference time-domain (FDTD) method. In both cases antennas (monopoles in 2-D and bowties in 3-D) were placed on a flattened breast model. Promising results were obtained. The work presented here follows the general approach in [3] and [4], and presents a preliminary numerical evaluation of a detection system more amenable to practical implementation. Thus, we believe that this new approach offers a feasible alternative to traditional microwave imaging for breast tumour detection.

Manuscript received July 23, 1999; revised September 7, 1999. This work was supported by NSERC.

The authors are with the Department of Electrical and Computer Engineering, University of Victoria, Victoria, BC V8W 3P6, Canada.

Publisher Item Identifier S 1051-8207(99)09819-0.

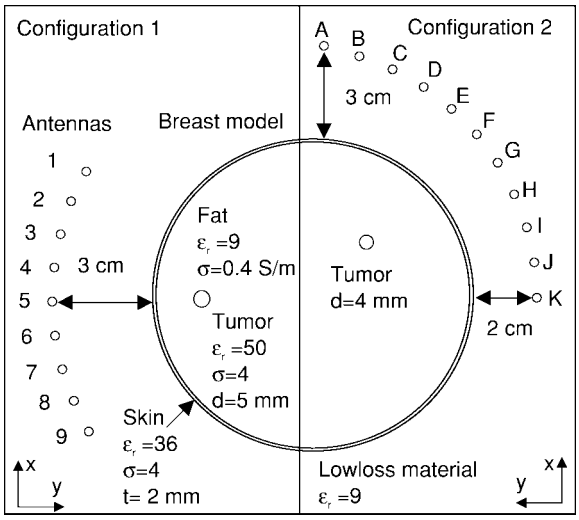

Fig. 1. Proposed system configuration. Configuration 1 (left): 9 antennas are placed concentric with the 10-cm-diameter breast model. A 5-mm-diameter tumour is located 1.25 cm under the skin. Configuration 2 (right): 11 antennas are positioned between 2 and 3 cm from the breast model. The tumor is 4 mm diameter and located 2 cm from the skin. In both cases, the electrical properties are as in [3], and the antennas are spaced circumferentially 1 cm apart.

II. Proposed System and Modeling

Our system is suitable for a routine scan of the breast, and its representation in one plane is shown in Fig. 1. The patient lies in a prone position with the breasts immersed in a liquid with electrical properties similar to those of fat. An array of antennas is placed in the liquid and positioned in an arc at a distance from the breast. For data acquisition, one antenna transmits an ultrawide-band pulse and the scattered returns are recorded at the same antenna. This is repeated sequentially for each antenna in the array. The antennas are spaced to reduce their coupling, however the array may be rotated to a new position for acquisition of additional data. Furthermore, translating the array vertically allows for scans of different cross sections through the breast.

This antenna configuration differs from that described in [3] and [4] in two ways. First, the array is placed sufficiently far from the skin so that returns from the breast do not arrive during pulse transmission. This allows for recording of skin reflections and their use in image processing. The antennas used here are resistively loaded dipoles of length 1.35 cm, while 8-cm-length bowties are presented in [4] and [5]. The smaller antennas are practical for implementation, as placement of an array of antennas near the breast is possible and results in shorter acquisition time due to electronic scanning of elements.

In this preliminary study, the breast is modeled as a finite cylinder with the electrical properties of fat surrounded by an

outer layer of skin. Tumors are modeled as small cylinders with the same length as the breast model. The model is immersed in a material with the same dielectric constant as fat but with very low conductivity. Material properties and dimensions are shown in Fig. 1. Although the breast model varies only in two dimensions (i.e., cross section does not change along the axis of cylinder), a full 3-D simulation is performed in order to model the antenna properly. In future, the incorporation of an appropriate 3-D breast model and the addition of a vertical scan with the antenna array to provide images of different cross sections will extend this to a full 3-D problem.

A resistively loaded Wu-King dipole [6] illuminates the breast model with a pulse, then records returns. The resistively loaded dipole is better suited to pulse radiation than a standard dipole and requires less computational effort than a bowtie. The antenna is excited with a differentiated Gaussian pulse

$$V(t) = (t - t_o)e^{-(t-t_o)^2/\tau^2} \tag{1}$$

where $\tau = 0.0625$ ns and $t_o = 4\tau$. The resulting signal has temporal duration (full-width half-maximum) of 0.17 ns and approximately 6-GHz bandwidth with maximum near 4 GHz, the frequency at which the Wu-King dipole is designed.

The FDTD method is used to simulate the operation of a single, resistively loaded antenna located between 2 and 3 cm from the breast model. Individual simulations used together represent an antenna scanned around the model or an array with sequentially pulsed elements (assuming minimal coupling between elements). All FDTD simulations are performed in 3-D. Graded mesh are used to increase the resolution close to the antenna (0.25 mm) and regions of the breast model near the antenna, while a resolution of 2 mm is used in the rest of the problem domain. Perfectly matched layers (parabolic profile, 8 layers, 60-dB attenuation) [7] are placed at a minimum distance of 3 cm from the antennas or breast model.

III. Tumor Detection Algorithms

The preliminary detection algorithm locates tumors in two dimensions. It is assumed that the breast cross section is circular, however models with noncircular contours will be considered in future work. The signal processing method involves calibration, subtraction of skin returns, correlation detection, and a synthetic scan of the focal point through the region of interest. First, the voltages recorded at each antenna are calibrated by subtracting previously obtained simulation results without an object present. The reflection from the thin layer of skin is the dominant signal component in the calibrated voltages. While returns from the skin provide useful information, these signals tend to obscure returns from the tumor. Thus, the second step in tumor detection involves reducing the initial reflection from the skin. An approximation to the skin reflection is formed using returns computed for a similarly sized (and located) solid cylinder of skin. Two time-shifted, scaled, and summed versions of the solid cylinder return are used to form this approximation, thus also providing an estimate of the skin location and thickness. This has been investigated and holds for various skin thicknesses, distances

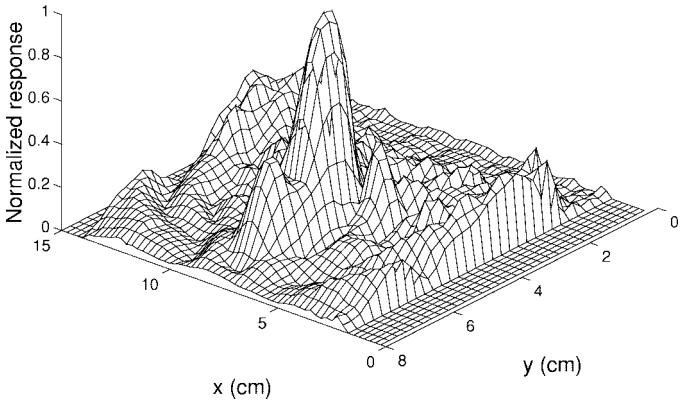

Fig. 2. Processed returns from antennas 2 to 8 of configuration 1 (left of Fig. 1). The maximum of the first peak is at $x = 8$ cm, $y = 4.6$ cm, while the tumor center is located at $x = 8$ cm, $y = 4.5$ cm.

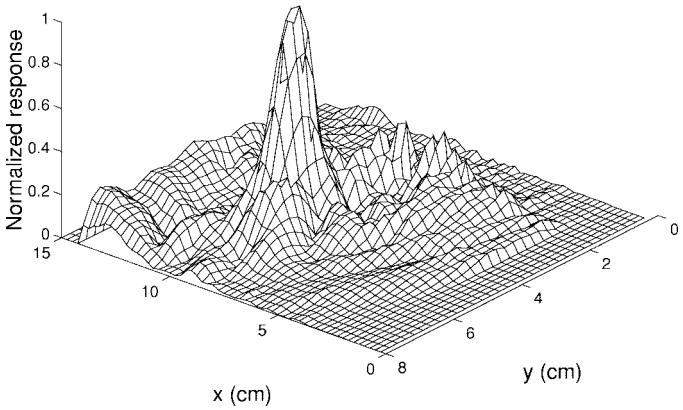

Fig. 3. Processed returns from antennas B to J of configuration 2 (right part of Fig. 1). The tumor center is located at $x = 9.8$ cm, $y = 4.6$ cm, and the peak in the figure is at $x = 9.8$ cm, $y = 4.8$ cm.

from the antenna and for models with tumors present. The approximate signal due to the skin is subtracted from the total recorded signal, greatly reducing the effect of the skin in tumor detection and image creation. These modified data are then correlated with the calibration voltage in order to enhance the tumor returns. The final step in tumor detection is similar to that in [3] and [4]. The focus is scanned through the region of interest in increments of 0.25 cm. Time delays, based on a first-order estimate of propagation through lossless fat, are applied to the signal recorded at each antenna. The delayed signals from each antenna are summed and averaged over a time window corresponding to 0.25 cm. The envelope of the data is displayed. It should be noted that signal analysis is performed after a complete breast scan (circumferential in this case, circumferential plus vertical in real application) has been obtained.

IV. Results

The effectiveness of the tumor detection algorithm is illustrated in Figs. 2 and 3. Fig. 2 shows results for the concentric breast object and antenna array on the left half of Fig. 1. The tumor response is clearly evident. Incomplete cancellations, related to calibration and skin subtraction, as well as multiple reflections are responsible for the less notable responses. Fig. 3

TABLE I
TUMOR RESPONSE FOR VARIOUS TUMOR SIZES AND LOCATIONS

Antenna to skin	Tumor diameter	Tumor depth	R_s(dB)	R_e (dB)
3 cm	5 mm	3.75 cm	-45.8	-104.5
	5	2.75	-39.2	-97.8
	5	1.25	-27.7	-86.4
	5	0.75	-23.5	-82.1
	2	3.9	-50.2	-108.9
	2	0.9	-24.8	-82.9
2 cm	4	2	-26.3	-82.2

shows results for the configuration on the right of Fig. 1, and also clearly indicates the presence of the tumor.

To further evaluate system performance, resolution and level of return from various tumors are investigated. Detection refers to ability to indicate the presence of a tumor, while resolution is related to uncertainty about the location and size. Resolution is of interest in two directions (x and y in Figs. 2 and 3). The slant-range (y) resolution is determined primarily by the bandwidth of the pulse, and is about 1 cm for the pulse used. The lateral (x) resolution is defined here as the extent of the full-width half-maximum response of the tumor at the maximum return position in the slant-range direction. With linear interpolation to the half-maximum point, attained resolutions with the antennas shown in Fig. 1 are about 1.3 cm for the 5-mm-diameter tumor and 1.1 cm for the 4-mm-diameter tumor. When the array is not centered about the tumor or an insufficient number of elements are included, the tumor response is not as clearly evident due to decreased magnitude of the response. Resolution does not dramatically improve with more antennas or more finely spaced antennas, perhaps due to the ultrawide-band nature of the signal [8]. However, the sidelobes of the response do decrease, increasing probability of detection.

The level of return from tumors of various sizes and locations provides insight into system requirements and performance. Table I examines the magnitude of peak-to-peak returns from various tumors recorded at a single antenna. The tumor response is compared to returns from the skin (R_s), and also to the excitation signal (R_e). Data in Table I indicate the feasibility of detecting tumors of diameter 2 mm at depth of 4 cm, given a receiver system with sufficient dynamic range.

V. CONCLUSIONS

This preliminary study indicates the feasibility of a new configuration for microwave breast tumor detection. The system is based on ideas similar to those of Hagness *et al.* [3], [4], however is more amenable to practical implementation. Results obtained with preliminary processing algorithms indicate the presence of tumors and their location. Detection of tumors with diameters greater than 2 mm and depths less than 4 cm appears feasible. Future work includes improvement of antennas, skin subtraction, imaging algorithms, and investigation of cross-polarization and frequency characteristics of tumors.

ACKNOWLEDGMENT

The authors wish to thank Dr. S. Hagness for many interesting discussions and her encouragement.

REFERENCES

[1] P. M. Meaney, K. D. Paulsen, and J. T. Chang, "Near-field microwave imaging of biologically-based materials using a monopole transceiver system," *IEEE Trans. Microwave Theory Tech.*, vol. 46, pp. 31–45, Jan. 1998.

[2] A. Franchois, A. Joisel, C. Pichot, and J.-C. Bolomey, "'Quantitative microwave imaging with a 2.45-GHz planar microwave camera," *IEEE Trans. Med. Imag.*, vol. 17, pp. 550–561, Aug. 1998.

[3] S. C. Hagness, A. Taflove, and J. E. Bridges, "Two-dimensional FDTD analysis of a pulsed microwave confocal system for breast cancer detection: Fixed-focus and antenna-array sensors," *IEEE Trans. Biomed. Eng.*, vol. 45, pp. 1470–1479, Dec. 1998.

[4] ———, "Three-dimensional FDTD analysis of a pulsed microwave confocal system for breast cancer detection: Design of an antenna-array element," *IEEE Trans. Antennas Propagat.*, vol. 47, pp. 783–791, May 1999.

[5] ———, "Wideband ultralow reverberation antenna for biological sensing," *Electron. Lett.*, vol. 33, pp. 1594–1595, Sept. 11, 1997.

[6] J. G. Maloney and G. S. Smith, "A study of transient radiation from the Wu-King resistive monopole—FDTD analysis and experimental measurements," *IEEE Trans. Antennas Propagat.*, vol. 41, pp. 668–676, May 1993.

[7] J. P. Berenger, "A perfectly matched layer for the absorption of electromagnetic waves," *J. Comput. Phys.*, vol. 114, pp. 185–200, 1994.

[8] H. Urkowitz, C. A. Hauer, and J. F. Koval, "Generalized resolution in radar systems," *Proc. IRE*, vol. 50, pp. 2093–2105, 1962.